*Physical Modelling in Geotechnics*


# Behaviour of sandy and clayey slopes exposed to artificial rain in small-scale model

Ž. Arbanas, J. Peranić, V. Jagodnik, N. Čeh, S. Pajalić & M.V. Prodan
*Faculty of Civil Engineering, University of Rijeka, Croatia*

**ABSTRACT:** Physical modelling of landslides by analysing the behaviour of small-scale landslide models subjected to artificial rainfall can be divided into modelling under 1g conditions and under increased acceleration (n times gravity) in a centrifuge. In this paper, the modelling of small-scale landslides on sandy and sandy-clayey slopes under 1g loading conditions under artificial rain will be discussed. The results obtained in small-scale sandy and sandy-clayey models at different slope inclinations exposed to different artificial rainfall will be presented, as well as the analyses of the factors affecting landslide initiation, propagation, and their relationship with the slope material, the infiltration process and the overall soil resistance in a slope related to soil strength, effective pressures and the contribution of matric suction in the unsaturated part of the slope.

**Keywords:** small-scale slope, rainfall, landslide, initiation, monitoring.

## 1 INTRODUCTION

Landslides are hazardous motions of a mass of rock, earth or debris down the slope (Cruden, 1991) that threaten vulnerable human settlements in different environments all around the World. An increase in the frequency and/or intensity of heavy rainfall due to changing climate significantly increases the risk of landslides in landslide-prone areas. Developments of human activity in mountainous and coastal areas, including the construction of transportation routes, expansion of urban areas and deforestation due to population growth and migration, increase exposure to the landslide hazard. The second most often triggering factors, strong earthquakes have the potential to initiate rapid landslides with long runout distances. The combined effects of both triggering factors can lead to greater impacts from catastrophic landslides such as debris flows, rock falls and mega slides.

Modelling of landslide initiation was based only on numerical modelling results using soil strength parameters obtained from soil laboratory testing in conventional laboratory apparatus for a long time. Physical modelling of landslide behaviour using small-scale models was introduced as a solution in different landslide researches in 1970s and 1980s in Japan (Oka 1972; Kutara and Ishizuka 1982) on natural slopes exposed to artificial rainfall. The laboratory experiments of landslide behaviour in a scaled physical models (known as flume or flume test) started from 1980s in Canada (Hungr and Morgenstern, 1984), Japan (Yagi et al., 1985) and Australia (Eckersley, 1990) under 1g conditions. Small scale landslide modelling under increased acceleration in geotechnical centrifuge was also successfully adopted (e.g. Kimura 1991; Take et al. 2004) but under circumstances of centrifuge limitations.

This paper discusses small scale landslide modelling in 1g loading conditions. The main task of landslide physical modelling was research of initiation, motion and accumulation of fast and slow slides caused by infiltration of rainfall in a slope and fluidification. This research was conducted within the Project "Physical modelling of landslide remediation constructions' behaviour under static and seismic actions" at the University of Rijeka, Croatia (Arbanas et al., 2019). The main objective of the Project is modelling and analysing behaviour of landslide remedial measures in physical models of scaled landslides under static (Arbanas et al., 2020) and seismic conditions. This paper presents the results of landslide initiation tests of sandy and clayey scaled slopes subjected to artificial rainfall. Landslide development was monitored by observing surface displacements using structure-from-motion (SfM) photogrammetry, terrestrial laser scanner (TLS) and a pair of high-speed cameras, and by observing landslide movements within the modelled displaced mass using accelerometers (Pajalić et al., 2021). Pore water pressure and soil moisture sensors were used to observe the hydraulic response of a slope.

## 2 MATERIALS AND METHODS

The physical model of a scaled slope was designed to enable initiation of a landslide caused by controlled artificial rainfall and equipped with adequate photogrammetric equipment and complex sensor network with ability to measure displacements, soil moisture and pore water pressures within a slope (Fig. 1) (Arbanas et al., 2020). Dimensions of the slope model are 1.0 m (width) x 2.3 m (length) x 0.5 m (height). The maximum depth of a soil material in the slope was adopted to be 30 cm. Slope inclination is adjustable from 20° to 45°. The series of tests described in this paper were carried out on slope inclinations of 35° degrees with two different types of soil as slope material.

To ensure the homogeneity of the soil material in the slope, two relatively simple materials were chosen to play the role of characteristic cohesionless and cohesive soils. The fine grained (0 – 0.1 mm) Drava River sand was chosen as the base material for the representation of cohesionless slopes. The second material is a mixture of the base material with 15% mass of industrial kaolin. Mass of 15% of kaolin was selected after a series of direct shear tests carried out on various sand-kaolin mixtures. The sand mixture with 15% of mass of kaolin clearly presented behaviour of fine-grained, cohesive materials with stable cohesion values. Friction angle and cohesion were determined in direct shear apparatus at the same relative density of 50% and at normal stresses similar to those in the slope model (4, 8 and 15 kPa). Hydraulic conductivity was determined using the falling head test in oedometer. The grain size distribution curves of the selected materials are presented in Fig. 2, while Table 1 presents the basic physical properties and initial conditions at the start of the tests. Slope materials were installed in the slope in 5 layers, each 6 cm thick to a total height of 30 cm.

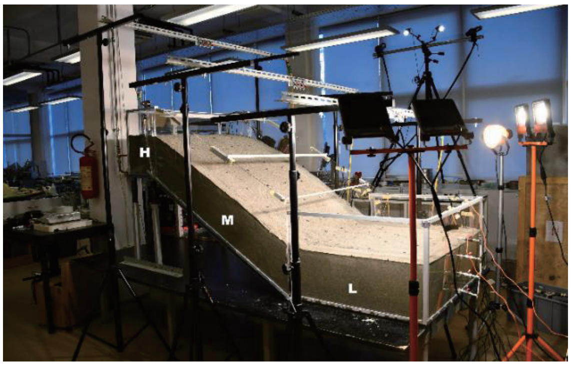


Fig. 1. Photo of the physical model (Arbanas et al., 2020; Peranić et al., 2022).

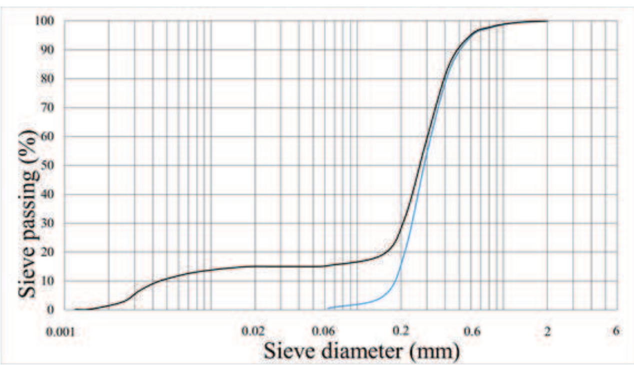


Fig. 2. Grain size distribution curves of the Drava River sand (blue) and sand-kaolin mixture with 15% of mass of kaolin (black).

Table 1. Basic physical properties of the Drava River sand and sand-kaolin mixture with 15% of mass of kaolin built-in the model and initial conditions at the start of the tests.

| Parameter | Symbol | Sand | Sand-kaolin mixture |
|---|---|---|---|
| Specific gravity | $G_s$ | 2.70 | 2.67 |
| Dry density | $\rho_d$ (g/cm$^3$) | 1.52 | 1.51 |
| Total density | $\rho_t$ (g/cm$^3$) | 1.55 | 1.63 |
| Effective particle size | $D_{10}$ (mm) | 0.19 | 0.056 |
| Effective particle size | $D_{60}$ (mm) | 0.37 | 0.207 |
| Uniformity coefficient | $c_u$ | 1.947 | 54.107 |
| Minimum void ratio | $e_{min}$ | 0.641 | 0.544 |
| Maximum void ratio | $e_{max}$ | 0.911 | 1.430 |
| Hydraulic conductivity | $k_s$ (m/s) | 1E-05 | 3.5E-06 |
| Friction angle | $\phi$ (°) | 34.9 | 31.7 |
| Cohesion | c (kN/m$^2$) | 0 | 4.4 |
| Initial porosity | $n_i$ | 0.44 | 0.434 |
| Initial void ratio | $e_i$ | 0.78 | 0.766 |
| Initial relative density | $Dr_i$ | 0.5 | 0.75 |
| Initial water content | $w_i$ (%) | 2 | 8.1 |

Prepared materials with a water content of w=2% and 8.1% were installed using the under-compaction method (Ladd, 1978). Each layer was compacted using the manual compactor to the medium dense conditions of relative density $D_r$=50%. In order to achieve homogeneity of the material in the slope and relatively uniform conditions in the built-up material, the model was built up in three segments (lower (L), middle (M) and upper (H) part).

The new rainfall simulator was constructed as part of the Project consisted of three sprinkler branches, each equipped with four different axial-flow full-cone nozzles with a spray angle of 45° or 60°. Each branch has been placed at such a height that the water can reach the edges of the plexiglass sides without creating too much water on the edges or outside of the model. This solution covers a wide range of rainfall intensities, from less than 30 l/h/m$^2$ to more than 140 l/h/m$^2$ at a reference pressure of 2 bar (Arbanas et al., 2020).

## 3 TEST RESULTS

After construction of the slope model and installing monitoring equipment within the slope, the slope models were exposed to artificial rainfall from three nozzles, one nozzle in each part of the slope (upper, middle and lower). Tests were conducted at the slopes built in sandy and sand-kaolin slopes at inclination of 35$^0$ and the applied rainfall intensities through the tests are presented in Fig. 3.

The slopes were exposed to different rainfall intensities: rainfall in the sandy slopes had intensities of 72.6 mm/h, while the slopes built of sand-kaolin mixture had intensities of 22.3 mm/h. The selection of rainfall intensities was based on infiltration conditions and the main requirement was that all the water at the point of contact on the model surface is infiltrated without forming surface runoff. The applied intensities were at the upper precipitation values that can be infiltrated in a soil without surface runoff.

After the initial establishment of a constant rainfall intensity and a stable infiltration process, the models were exposed to rainfall at the constant intensities until the slope failed or until the end of the test. Tests were continued until the retrogressive slides reached the top of the slope (Fig. 4a). The time from the rainfall start to the first signs of instability (cracks) in the slope foot was relatively long (62 minutes), while the retrogressive development to the top of the slope occurred in the following 30 minutes.

In test conducted on slopes with sand-kaolin mixture, the failure mechanism was completely different from observed in sandy slope. Although the rainfall intensities were significantly lower than the intensities on sandy slopes, the first signs of sliding appeared relatively quickly after the rainfall start (35 minutes). After appearance of the first cracks, the further retrogressive landslide development occurred to the top of the slope. This development was without significant movements in the slope; just new tension cracks were opened. The new stage occurred at the moment when the ground water level reached the slope surface in the middle part of the slope and forming small springs and surface flows (Fig. 4b). At this moment, the joint mechanism of sliding and surface erosion started with a relatively fast retrogressive instability development up the top of the slope.

The occurred superficial signs of sliding initiations and the causes for their occurrence can be explained by results of the continuous volumetric water content monitoring (Fig. 5). Sensors measuring volumetric water content were installed at four different depths (6, 12, 18 and 24 cm below the slope surface) in the lower (L), middle (M) and upper (H) parts of the slope (Fig. 5).

After analysis of the measured results, the landslide processes could be explained as it follows. (i) In the sandy slope, with relatively high hydraulic conductivity, the volumetric water content increases due to infiltration until saturation in the deepest part of the slope, forming the water table. As it established, a flow down the slope started causing a rapid rise in the groundwater level in the lower part of the slope. This led to decrease in the soil shear strength with complete loss of matric suction, failure and further retrogressive landslide development to the top of the slope. (ii) In slopes made of sand-kaolin mixture, with significantly lower hydraulic conductivity, the process of saturation occurred firstly in the surface layer that caused an increase of the weight of surface layer causing cracks and shallow instabilities in the middle part of the slope without significant movements. The opening of the cracks allowed the water to penetrate in deeper layers and form separated saturated zones in the slope, but the matric suction remains maintained in the most parts of the slope. In some isolated local zones, near existing cracks, the ground water level rises to the surface causing springs and surface flows.

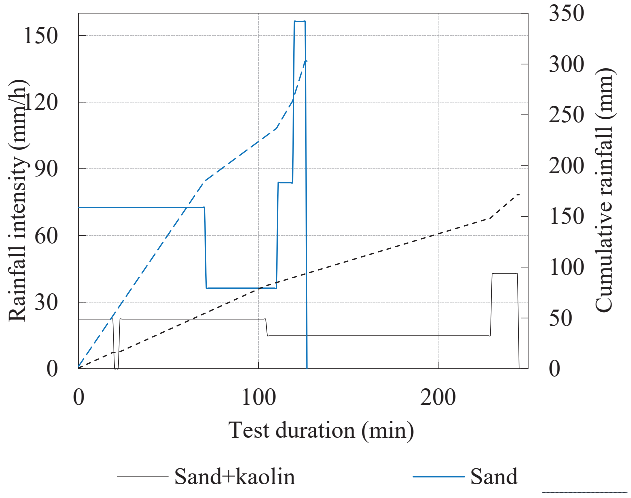


Fig. 3. Simulated rainfall in tests on sandy slope (blue) and slope of mixture of sand with 15% of kaolin (black).

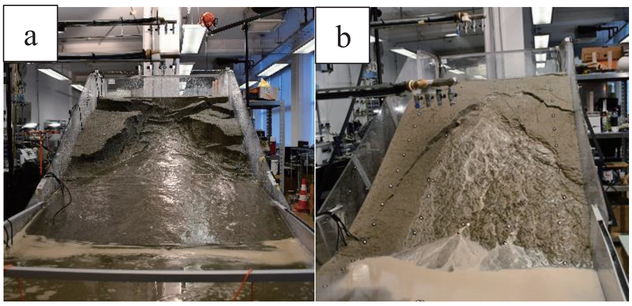


Fig. 4. Photos of instabilities in small-scale slope model: a) Sandy slope (left); b) Sand-kaolin mixture slope (right)

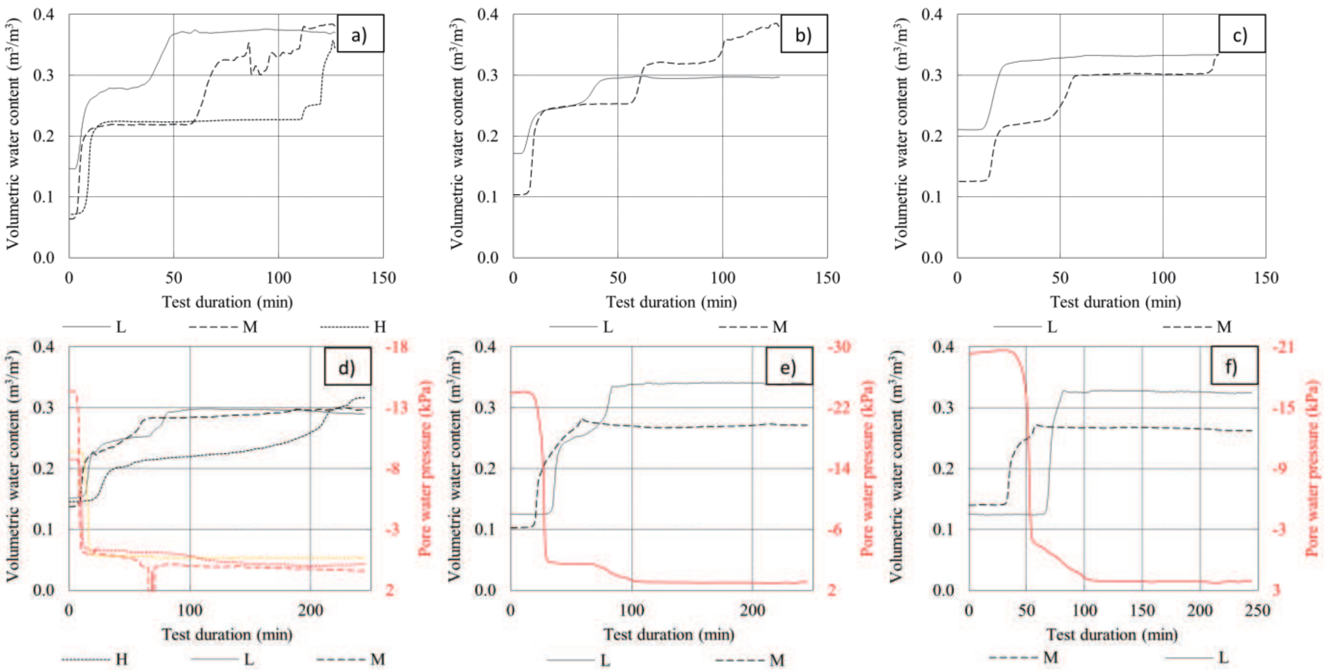

Fig. 5. Volumetric water content and pore water pressure measurements: Upper row clean sand slope (35° inclination) at 6 cm (a), 12 cm (b) and 24 cm (c) from the slope surface; Lower row mixture of sand with 15% of kaolin at 6 cm (d), 12 cm (e) and 24 cm (f) from the slope surface in upper (H), middle (M), and lower (L) part of the slope.

## 4 CONCLUSIONS

This paper presents the results of landslide initiation in small-scale slopes built of sand and sand-kaolin mixture and exposed to artificial rainfall. The results of tests conducted on these two types of materials at the same slope angles are presented. The observed failure mechanisms are described and explained, as well as the infiltration process based on the results of volumetric water content measurements. Besides the results presented in this paper, several additional measurements have been carried out during the tests and are still being analyzed. The results obtained by geodetic monitoring and the observations of surface movements should complete the analyses carried out, will play an important role in fully explanation of the landslide process.

## ACKNOWLEDGEMENTS

This research was funded by Croatian Science Foundation under the Project IP-2018-1503 Physical modelling of landslide remediation constructions behaviour under static and seismic actions. This support is gratefully acknowledged.

## REFERENCES

Arbanas, Ž., Jagodnik, V., Peranić, J., Pajalić, S., Prodan, M.V. and Čeh, N. 2020. Physical Model of Rainfall Induced Landslide in Flume Test: Preliminary Results. *Proceedings of European Conference of Physical Modeling in Geotechnics*, p. 8.

Arbanas, Ž., Pajalić, S., Jagodnik, V., Peranić, J., Vivoda Prodan, M., Đomlija, P. and Dugonjić Jovančević, S. 2019. Development of physical model of landslide remedial constructions' behaviour. *Proceedings of the 4th Regional Symposium on Landslides in the Adriatic - Balkan Region*, Bosna and Herzegovina Geotechnical Society, pp. 103–108.

Cruden, D.M. 1991. A simple definition of a landslide. *Bulletin of the International Association of Engineering Geology* 43 (1), 27–29.

Eckersley, D. 1990. Instrumented laboratory flowslides. *Géotechnique* 40 (3), 489–502.

Hungr, O. and Morgenstern, N.R. 1984. Experiments on the flow behaviour of granular materials at high velocity in an open channel. *Geotechnique* 34 (3), 9.

Kimura, T. 1991. Failure of fills due to rain fall. Centrifuge, Balkema, pp. 509–516.

Kutara, K. and Ishizuka, H. 1982. Seepage flow in the embankment and stability of slope during rain (in Japanese). *Tsuchi-to-kiso,* Paper No 1330.

Ladd 1978. Preparing Test Specimens Using Undercompaction. *Geotechnical Testing Journal* 8.

Oka, H. 1972. Impacts by the "artificial landslide": re-examine the rage of nature (in Japanese). *Kagaku Asahi* 32 (1), 152–153.

Pajalić, S., Peranić, J., Maksimović, S., Čeh, N., Jagodnik, V. and Arbanas, Ž. 2021. Monitoring and Data Analysis in Small-Scale Landslide Physical Model. *Applied Sciences* 28.

Peranić, J., Jagodnik, V., Čeh, N., Pajalić, S., Jagodnik, P. and Arbanas, Ž. 2022. Landslide initiation in small-scale sandy and clayey slopes exposed to artificial rain. *Proceedings of the 20th International Conference on Soil Mechanics and Geotechnical Engineering,* Australian Geomechanics Society, pp. 1075-1080.

Take, W.A., Bolton, M.D., Wong, P.C.P. and Yeung, F.J. 2004. Evaluation of landslide triggering mechanisms in model fill slopes. *Landslides* 1 (3), 173–184.